Detection and partial characterization of a putative closterovirus affecting Ficus carica: *molecular, ultrastructural and physiological aspects of infected leaves*

Khalaf Ali Fayez & Sabry Younis Mahmoud

Acta Physiologiae Plantarum

ISSN 0137-5881
Volume 33
Number 6

Acta Physiol Plant (2011) 33:2187-2198
DOI 10.1007/s11738-011-0758-0

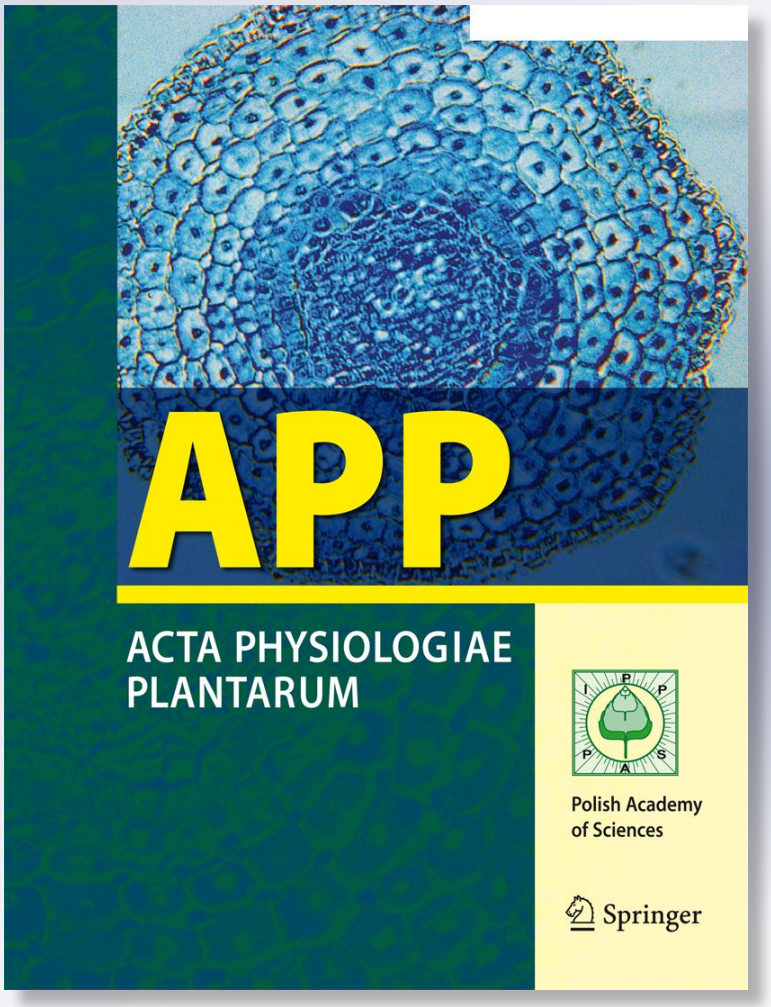

Springer

Acta Physiol Plant (2011) 33:2187–2198
DOI 10.1007/s11738-011-0758-0

ORIGINAL PAPER

Detection and partial characterization of a putative closterovirus affecting *Ficus carica*: molecular, ultrastructural and physiological aspects of infected leaves

Khalaf Ali Fayez · Sabry Younis Mahmoud

Received: 4 September 2010 / Revised: 15 March 2011 / Accepted: 28 March 2011 / Published online: 20 April 2011

Abstract *Fig mosaic disease* (FMD) was systemically transmitted to susceptible fig plants by grafting and led to development of symptoms including a wide array of discoloration, green blisters, mottling, crinkling and deformation of leaves and fruits. A sensitive assay for the detection of FMV using specific enzyme-linked immune sorbent assay and reverse transcription-polymerase chain reaction was developed. A double-stranded RNA ca. 19 kbp in size was obtained from the fig tissue extract and used as a template. A cDNA fragment (350 bp) of phosphate motifs 1 and 2 of the heat shock-protein 70 homologue of the family Closteroviridae was amplified using a specific primer set. Virions were flexuous filaments up to 1,800 nm in length and ~21 nm in diameter. Viral infection formed new polypeptides in leaves that reflect pathogen-related proteins. Total photosynthetic pigment contents of virus-infected leaves decreased by 33.06%, with a raise in chl *a*/*b* ratio that was mainly caused by a decline in chl *b* content. Chloroplasts of virus-infected leaves lost their envelopes, and the internal structures of grana and stroma thylakoids were deformed and turned to spherical shapes. No virus inclusion bodies were detected in chloroplasts or other mesophyll cell organelles. Starch grains of chloroplasts were absent in the virus-infected leaves. Viral infection caused a decline in catalase and induction in peroxidase activities in leaves. Levels of thiobarbituric acid reactants in viral-infected leaves increased by 15%, while the content of total phenolics increased by 29%, in respect to healthy ones. The present results indicate a possible presence of *Fig leaf mottle-associated virus-1* (FLMaV-1) in fig trees and provide an overview of the negative effects on fig leaves in response to FLMaV-1 infection from morphological, physiological and subcellular perspectives.

Keywords *Ficus carica* · *Fig leaf mottle-associated virus-1* · Pigments · Ultrastructure · Antioxidant compounds

Abbreviations

CAT	Catalase
Chl	Chlorophyll
cDNA	Complementary deoxy ribonucleic acid
dsRNA	Double-stranded RNA
ELISA	Enzyme-linked immune sorbent assay
FLMaV-1	Fig leaf mottle-associated virus-1
FMD	Fig mosaic disease
FMV	Fig mosaic virus
Hsp70h	Heat shock-protein 70 homologue
MDA	Malondialdehyde
PSII	Photosystem II
POX	Peroxidase
ROS	Reactive oxygen species
RT-PCR	Reverse transcription-polymerase chain reaction
TBARS	Thiobarbituric acid reactants

Communicated by B. Barna.

K. A. Fayez (✉)
Biology Department, Faculty of Science,
Taif University, Taif, Saudi Arabia
e-mail: khalaffayez@yahoo.com

K. A. Fayez
Botany Department, Faculty of Science,
Sohag University, Sohag, Egypt

S. Y. Mahmoud
Agricultural Microbiology Department,
Faculty of Agriculture, Sohag University, Sohag, Egypt

Introduction

Ficus carica L., a deciduous tree belonging to the Moraceae family is very common in the Mediterranean basin and in countries with a dry and sub tropical climate (Mars 2003; Stover et al. 2007). Fig tree plantations cover a 427,000 ha area worldwide with an overall yield of million tons. The largest fig producing countries are Turkey, Egypt, Iran, Greece and Algeria (FAO 2006). *Ficus carica* fruit is a famous fig of commerce well known for its nutritive value and is consumed fresh or dry (Veberic et al. 2008).

The Closteroviridae is one of the most diverse families which comprises more than 30 plant viruses with flexuous filamentous virions of 700–2,000 nm in length and 12 nm in diameter that contain the mono-, bi- or tripartite positive strand single-stranded RNA genomes that range in size from over 15 to almost 20 kb (Karasev 2000; Tzanetakis and Martin 2007). The family is divided into three genera based on genome organization: *Ampelovirus*, *Closterovirus* and *Crinivirus*. Several members of the family cause devastating diseases (Karasev 2000). *Fig leaf mottle-associated virus-1* (FLMaV-1) is a putative member of the genus *Closterovirus* (Elbeaino et al. 2006). Fig mosaic is a ubiquitous disease possibly caused by several different viruses including FLMaV-1, which is transmitted by grafting and, in nature, by the eriophyd mite *Aceria ficus* (Serrano et al. 2004; Elbeaino et al. 2006, 2007, 2009a, b; Walia et al. 2009).

The aetiology of the disease is still uncertain. Isometric and filamentous virus particles have been observed occasionally in thin-sectioned tissues of symptomatic leaves of fig from Italy and England (Martelli et al. 1993; Appiano et al. 1995). Leaf dips of parenchymal cells of infected fig leaves showed the presence of filamentous closterovirus-like particles with distinct cross banding and a length from 1,800 to 2,100 nm (Elbeaino et al. 2006, 2007).

Chloroplasts are more sensitive than other cell organelles to viral infection (Hernández et al. 2004). Concomitant with alteration in structure and function of chloroplasts, a sharp decline in photosynthesis occurs leading to cell death (Buchanan-Wollaston 1997). Deterioration of chloroplast structure, pigment composition and electron transport could be attributed to the damage caused mostly in photosystem II (PSII) during virus infection (Reinero and Beachy 1989; Rahoutei et al. 2000).

Various enzymes of antioxidant systems such as catalase and peroxidase participate in counteracting reactive oxygen species (ROS) produced during pathogen attack (Bolwell et al. 2002). Catalase (EC 1.11.1.6) activity increased in leaves of *Dactylis glomerata* L. infected with *Cocksfoot mottle virus* (CFMV) for the first 5 days following inoculation and then declined (Li and Burritt 2003). Activities of catalase (CAT), glutathione reductase (GR) and superoxide dismutase (SOD) of *Phaseolus vulgaris* leaves rapidly declined following inoculation with *white clover mosaic virus* (WCMV), while total peroxidase activities increased (Clarke et al. 2002). Peroxidase (EC 1.11.1.7) activity usually increases in viral-infected plant tissues as reported in *Cucurbita pepo* plants infected with *cucumber mosaic virus* (CMV) and *zucchini yellow mosaic virus* (ZYMV) (Técsi et al. 1996; Radwan et al. 2007). Stimulation of peroxidase activity is greatest in resistant hosts that react with hypersensitivity (HR), although, increased activity has also been reported in susceptible hosts permitting systemic infection (Candela et al. 1994; Milavec et al. 2001).

Malondialdehyde (MDA) content is widely used to measure the extent of lipid peroxidation as an indicator of oxidative stress and membrane damage (Lin and Kao 2000). Radwan et al. (2006) reported an elevated amount of MDA in *C. pepo* leaves in response to ZYMV infection.

Phenolic compounds are secondary metabolites that are quite widespread in plants and can act as free radical scavengers and protect cells from oxidative toxicity (Léon et al. 1995; Costa et al. 2009; Oliveira et al. 2009). Viral infection induces phenolic deposits in infected wheat plants (Kofalvi and Nassuth 1995). It has been reported that the greater total phenolic content of the plant resulted in increased antioxidant capacity (Cai et al. 2004).

In the present work, physiological and molecular studies were done on the infected leaves of the common *F. carica* cv. Sultani. Data on virus identification as well as effects of infection on molecular, ultrastructural and physiological properties of host plants are fragmentary. The main objectives of this work were; (1) identification of the causal virus associated with the chlorotic mottling of fig plants; (2) determining the localization of causal virus in host cells by electron microscopy and (3) studying the cytopathic effects, ultrastructural and physiological alterations in leaves caused by virus infection.

Materials and methods

Viral isolation and identification

To study the distribution of the disease, 90 samples of naturally infected fig leaves were collected from 90 trees of 10 orchards. The chosen ten orchards of fig trees are located in Kafr El-Sheikh Governorate (Baltim region, three orchards), Sohag Governorate (Farm of Faculty of Agriculture, four orchards) and Qina Governorate (private sector, three orchards). The study was a survey on fig mosaic disease associated with fig trees and eriophyd mites in the ten orchards, which were selected randomly. The virus isolate was identified biologically, serologically and electron microscopically. The mite was identified in Pests and Plant Protection Department, National Research Center (NRC), Egypt.

Mechanical transmission

Tissues from young strongly symptomatic leaves of *F. carica* cv. Sultani were macerated in a mortar in the presence of 0.05 M phosphate buffer containing 2.5% nicotine. The resulted homogenate was then used with mechanical inoculation of carborundum-600 and dusted on the leaves of *Chenopodium amaranticolor*, *C. album*, *C. quinoa*, *Gomphrena globosa*, *Datura metal*, *D. stramonium*, *Nicotiana glutinosa*, *N. tabacum var. White Burley*, *Zinnia elegans* and *Cucumis sativus*. Inoculated plants were kept in a greenhouse and observed for symptom expression and tested for the presence of FM approximately 1 month after inoculation.

Grafting transmission

Double graft experiments (Fig. 2a, b) were carried out in a greenhouse to determine a grafting transmission and the resistance of *F. carica* cv. Kadota. One-year-old of potted symptomatic rooted cuttings from naturally infected *F. carica* cv. Sultani were used as rootstocks. The rootstocks were declared positive only after obtaining a positive reaction by indirect-enzyme-linked immune sorbent assay (ELISA), reverse transcription-polymerase chain reaction (RT-PCR), accompanied with the observation of the visual symptoms. Healthy shoots of *F. carica* cv. Kadota (Fig. 2a [first grafting, section 1)] were grafted unto infected rootstocks of cv. Sultani. One year later, healthy shoots of cv. Sultani were grafted onto the section 1 of cv. Kadota shoots (second grafting, section 2). The other subsequent double graft experiment (Fig. 2b) was carried out with the infected cv. Sultani (rootstock), healthy cv. Sultani (first grafting, section 1) and healthy cv. Sultani shoot (second grafting, section 2).The healthy rootstocks were used as controls (uninfected).

Eight replicates of double grafting plants succeeded. After 4 months of the second grafting, the grafted plants were verified visually for viral symptoms on rootstock, section 1 and section 2. Inoculation efficiency and the infection status of plants were verified by ELISA according to Clark and Adams (1977) to confirm the presence or absence of an FLMaV-1-like agent. Polyclonal antibodies were kindly provided by Dr. M.I. Salama [Agriculture Genetic Engineering Research Institute (AGERI), Egypt. Antibodies were raised against FLMaV-1.

Purification

Young leaves of grafted plants with petioles from symptomatic fig trees were collected from Sultani cultivar plants after grafting transmission. One hundred grams of leaves was homogenized in 100 mL of 0.1 M citrate buffer, pH 6.5, containing 0.1% β-mercaptoethanol. The extracts were filtered through four layers of cheesecloth and centrifuged for 20 min at 10,000 rpm. Triton X-100 (20%) was added to the supernatant and centrifuged at 35,000 rpm through a pad of 20% sucrose for 2 h. The pellet was suspended in 5 mL of 0.05 M Na_2PO_4 buffer pH 7.0. Further purification was carried out by the methods of Falk and Tsai (1984). Centrifugation in linear 10–40% (v/v) sucrose density gradients at 24,000*g* in a Beckman 28.1 rotor was performed for 3 h. The columns were fractionated manually in Eppendorf tubes (1 mL/tube) and subjected to spectrophotometry at 245 nm. Fractions which showed virus-like peaks were collected, diluted and centrifuged at 75,000*g* in a Beckman SN-2407 rotor for 2 h. Pellets were resuspended in 0.1 M borate buffer, pH 8.2. The resulted suspension was examined by electron microscopy (microscopy unit, NRC, Egypt).

Nucleic acid extraction

Total nucleic acids (TNA) were extracted from fig leaf veins of cv. Sultani, The tissue (100 mg) was extracted in 1 mL grinding buffer (4.0 M guandine thiocyanate; 0.2 M NaOAc, pH 5.2; 25 mM EDTA; 1.0 M KOAc and 2.5% w/v PVP), then TNA were fractionated by column chromatography on non-ionic cellulose (CF-11, Whatman). After fractionation, DNA and single-stranded RNA were digested by incubation for 30 min at 37°C according to Saldarelli et al. (1994). After additional phenol–chloroform extraction and centrifugation at 9,000*g* for 10 min, double-stranded RNA (dsRNA) was precipitated with ethanol and electrophoresed in 1.5% agarose gel in TAE buffer pH 7.8 (89 mM Tris–Acetate–EDTA). The gel was stained with ethidium bromide and visualized by a UV-transilluminator.

Reverse transcription-polymerase chain reaction

Two specific primers based on published sequence data of phosphate motifs 1 and 2 of *Fig leaf mottle-associated virus-1* (FLMaV-1) HSP70h protein gene, described by Elbeaino et al. (2006) were used for amplification of the FLMaV-1 HSP70h protein gene (approximately 350 bp). The sequences of the forward and reverse primers were 5′-CGT-GGC-TGA-TGC-AAA-GTT-TA-3′ (20 nt) and 5′-GTT-AAC-GCA-TGC-TTC-CAT-GA-3′ (20 nt), respectively. TNA were isolated according to (Harper and Kreamer 1995) from symptomless and symptomatic rootstocks, section 1 and 2 of grafted fig trees. One-step RT-PCR was performed using the Titan One Tube RT-PCR system (Roche Applied Science, Mannheim, Germany). Briefly, 25 µL of each Master mix 1 (4 µL of 0.2 mM dNTPs, 2 µL of 0.4 µM reverse primer, 2 µL

of 0.4 μM forward primer, 1 μL of extracted TNA, 2.5 μL of 5 mM DTT solution, 1 μL of 10 U RNAsin and 12.5 μL sterile double distilled water) and Master mix 2 (10 μL of 5 × RT-PCR buffer with 1.5 mM $MgCl_2$, 1 μL Enzyme mix [reverse transcriptase-Avian myloblastosis virus (AMV) and *Taq* DNA polymerase] and 14 μL of sterile double distilled water were added to a 0.2 mL thin-walled PCR tube (nuclease free) on ice. PCR tubes were transferred to the thermocycler set at 39°C for 1 h for the reverse transcription step, another thermocycler for PCR was programmed for one cycle with 94°C for 4 min and followed by 35 cycles with 94°C for 30 s, 58°C for 30 s, and 72°C for 40 s. Final extension was at 72°C for 7 min. Aliquots of 5 μL from each RT-PCR amplified product (cDNA) were analyzed by electrophoresis on 1.5% agarose gels in TAE buffer and then visualized by staining with ethidium bromide.

Leaf protein gel electrophoresis

SDS-PAGE was performed using 10% acrylamide gels according to the procedure of Laemmli (1970). Protein samples were extracted by grinding 1 g of fresh leaves in 0.5 ml of Tris–HCl buffer (0.2 M) in a pre-cooled mortar and pestle. Centrifugation was at 14,000 rpm at 4°C for 30 min. Supernatants (about 25 μg proteins) were mixed with an equal volume of buffer containing 0.125 M Tris–HCl, pH 6.8, 4% SDS, 20% glycerol, and 10% 2-mercaptoethanol and bromophenol blue as tracking dye. The prepared mixture was heated in water bath for 3 min at 96°C and loaded onto gel for 6 h at 10°C in running buffer containing 0.025 M Tris–HCl, 0.192 M glycine and 0.1% SDS. Bands of protein were visualized using 0.1% Commassie Brilliant blue R250 in a staining solution. Finally the gels were destained in a solution containing 40% (v/v) methanol, 7% glacial acetic acid and 53% distilled water.

Pigment analysis

The pigments were extracted from fig leaves with 80% acetone. Chl *a*, chl *b* and carotenoids were quantitatively determined spectrophotometrically at wavelengths 663, 647 and 470 nm, respectively, according to the equations of Lichtenthaler (1987).

$$\text{Chl } a = 12.25A_{663} - 2.79\ A_{647}$$

$$\text{Chl } b = 21.50A_{647} - 5.10\ A_{663}$$

$$\text{Carotenoid} = (1000A_{470} - 1.82\ \text{Chl } a - 95.15\ \text{Chl } b)/225$$

The concentrations for Chl *a*, Chl *b*, and the sum of leaf carotenoids (xanthophylls and carotenes) were expressed as mg g^{-1} fresh leaves.

Electron microscopy

Negative staining

Dips in 2% aqueous phosphotungstic acid (PTA) stain were made from leaf petioles and blades in carbon backed, parlodin-coated grids. Purified suspensions of infected fig leaves were mixed with 2% phosphotungstic acid-stain (1/1 v). Grids were floated on droplets of stain-suspension mixture. After 2 min, the excess fluid was removed by filter paper. Specimens were air dried and viewed by electron microscopy.

Leaf ultrastructure

Fresh leaf samples were fixed in 3% glutaraldehyde prepared in 0.05 M phosphate buffer (pH 7), at field sites for 3 h. Samples were rinsed several times in 0.05 M phosphate buffer and then were post fixed with 1% OsO_4 in 0.05 M phosphate buffer for 2 h. Samples were rinsed several times with 0.05 phosphate buffer and taken to the laboratory. Samples were then dehydrated in a gradient acetone series, and embedded in Spurr's (1969) medium. Ultrathin sections (60–70 nm thick) were stained with uranyl acetate and lead citrate. Specimens were viewed with a Jeol-1010 transmission electron microscope at 100 kV (Unit of Electron Microscopy at Sohag University, Egypt).

Antioxidant enzyme estimations

The activity of CAT (EC 1.11.1.6) was measured according to the method of Chandlee and Scandalios (1984) with some modifications. The assay mixture contained 2.6 mL of 50 mM potassium phosphate buffer (pH 7.0), 0.4 mL of 15 mM H_2O_2, and 0.04 mL of crude enzyme extract. The decomposition of H_2O_2 was followed by the decline in absorbance at 240 nm. The enzyme activity was expressed in units, where one unit of catalase converts 1 μmole of H_2O_2 min^{-1} g FW (U = 1 mM of H_2O_2 reduction min^{-1} mg^{-1} FW).

The activity of peroxidase (POX, EC 1.11.1.7) was measured by following the change in the absorption due to guaiacol oxidation ($E = 26.1\ mM^{-1}\ cm^{-1}$ min) at 470 nm according to Polle et al. (1994). The activity was assayed for 1 min in a reaction solution (3 mL final volume) composed of 100 mM potassium phosphate buffer (pH 7.0), 20 mM guaiacol, 10 mM H_2O_2 and 50 μL of crude extract. Enzyme activity was calculated in terms of μM of guaiacol oxidized min^{-1} g FW.

Lipid peroxidation

Malonyldialdehyde (MDA) content was determined as an indication of leaf lipid peroxidation according to

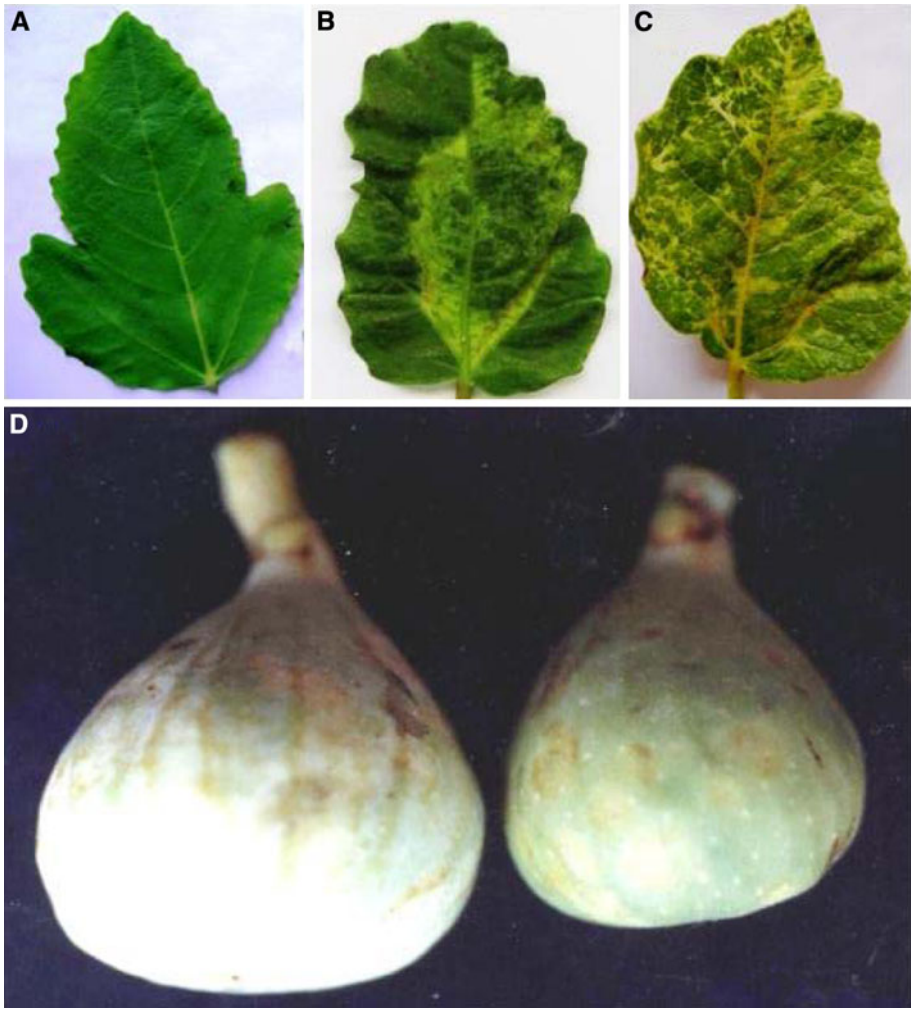

Fig. 1 Symptoms of fig mosaic virus in leaves (**b**, **c**) and fruits (**d**) of *Ficus carica* cv. Sultani infected with fig mosaic virus, healthy leaf (**a**)

Hernández and Almansa (2002). Fresh leaf samples (500 mg) were homogenized in 5 mL of 0.1% trichloroacetic acid (TCA). The homogenate was centrifuged at 15,000*g* for 20 min at 4°C. A 1 mL aliquot of the supernatant was mixed with 3 mL of 0.5% thiobarbituric acid (TBA) prepared in 20% TCA, and incubated at 90°C for 20 min. After stopping the reaction in an ice bath, samples were centrifuged at 10,000*g* for 5 min. The supernatant absorbance at 532 nm was then measured. After subtracting the non-specific absorbance at 600 nm, MDA concentration was determined using the extinction coefficient 155 mM^{-1} cm^{-1}.

Total phenolics

Total phenolics were measured with the Folin-Ciocalteu reagent (Dai et al. 1994). Twenty-five microlitres of the extracts was mixed with 110 µL Folin-Ciocalteu reagent,

Table 1 Survey of fig mosaic virus-disease at selected fig orchards

Governorate regions and orchard no.	Irrigation and fertilization	Mite	Average of viral infection (%)
Kafr El-Sheikh			
1	+	+	24
2	−	+	0.0
3	−	+	1.0
Sohag			
1	+	+	33
2	+	+	28
3	+	+	25
4	+	+	36
Quina			
1	+	+	19
2	+	+	32
3	+	+	26

Table 2 Symptoms on leaves of host range indicator plants inoculated with FLMaV-1 isolate

Host plants	Transmission (%)		Symptoms
	Mechanical	Grafting	
F. carica cv. White Aswan	0.0	100	LCS, M
F. carica cv. Sultani	0.0	100	LCS, M, Mal
F. carica cv. Kadota	0.0	0.0	–
Chinopodium amaranticolor	0.0	nd	–
C. quinoa	0.0	nd	–
C. album	0.0	nd	–
Nicotiana glutinosa	0.0	nd	–
N. tabacum var. white burley	0.0	nd	–
Datura metal	0.0	nd	–
D. stramonium	0.0	nd	–
Gomphrena globosa	0.0	nd	–
Zinnia elegans	0.0	nd	–
Cucumis sativus	0.0	nd	–

LSC light chlorotic spots, *M* mottling, *Mal* malformation, *nd* not detected, – no symptoms

200 µL 20% sodium carbonate and 1.9 mL distilled water, and placed at 60°C for 30 min. Optical density was measured with a spectrophotometer (Spekol Carl-Zeiss spectrocolorimeter, Germany) at 750 nm. A standard curve was constructed with different concentrations of gallic acid. The results were expressed as mg of gallic acid g^{-1} DW.

Results and discussion

Survey of fig mosaic disease and host range

The partial characteristics of a putative closterovirus affecting fig plants in Egypt were identified in the present study. *Ficus carica* cv. Sultani and white Aswan were susceptible to inoculation by the identified virus, while *F. carica* cv. Kadota was resistant. Nine of the chosen ten orchards of fig trees (*F. carica* cv. Sultani), grown in different regions in Egypt, showed varying patterns of chlorotic mottling and deformation of leaves (Fig. 1b, c) in comparison with the uninfected leaves (Fig. 1a). Pale yellow ring spots appear on the fruits (Fig. 1d), which turned dark blotches. Sometimes, the pale-yellow spots disappeared during maturation. Flecks spread and formed grooved depression on fruits and premature fruit dropped with severe infections. A mosaic symptom was observed visually on fig tree leaves and its prevalence was ranged from 1.0 to 36% in the infected trees of nine orchards (Table 1); however, the mosaic symptom was not visible in the trees of Baltim orchards grown in Kafr El-Sheikh governorate. Increasing mosaic symptoms were correlated with increasing soil irrigation and fertilization and its prevalence ranged from 19 to 36% (Table 1). In contrast, in Baltim region (Kafr El-Sheikh governorate), the fig trees grown in sandy mountains (poorly soil and low water contents), the mosaic prevalence (Table 1) was very low (0.0–1.0%).

Table 3 ELISA values, reactions and visual symptoms of tissue extracts of infected rootstock cv. Sultani, cv. Kadota grafted onto infected rootstocks (section1) and cv. Sultani grafted onto cv. Kadota (section 2)

Double graft experiment	Status	Indirect-ELISA		Visual symptoms
		Values at (A_{405nm})	Reaction	
Rootstock (cv. Sultani)	Infected	1.113 ± 0.016	+	+
	Healthy	0.212 ± 0.006	–	–
Section 1				
cv. Kadota	Infected	0.235 ± 0.007	–	–
	Healthy	0.221 ± 0.003	–	–
cv. Sultani	Infected	1.059 ± 0.007	+	+
	Healthy	0.236 ± 0.005	–	–
Section 2 (cv. Sultani)				
1A	Infected	0.219 ± 0.003	–	–
	Healthy	0.215 ± 0.003	–	–
2B	Infected	0.984 ± 0.003	+	+
	Healthy	0.226 ± 0.004	–	–
Positive control 10^{-1}		1.126 ± 0.003	+	
Negative control 10^{-1}		0.213 ± 0.004	–	

ELISA values are means of three replicates ± SD. (1A): section 2, *F. carica* cv., Sultani grafted onto *F. carica* cv. Kadota; (2B): section 2, *F. carica* cv. Sultani grafted onto *F. carica* cv. Sultani

+ positive, symptomatic; – negative, symptomless

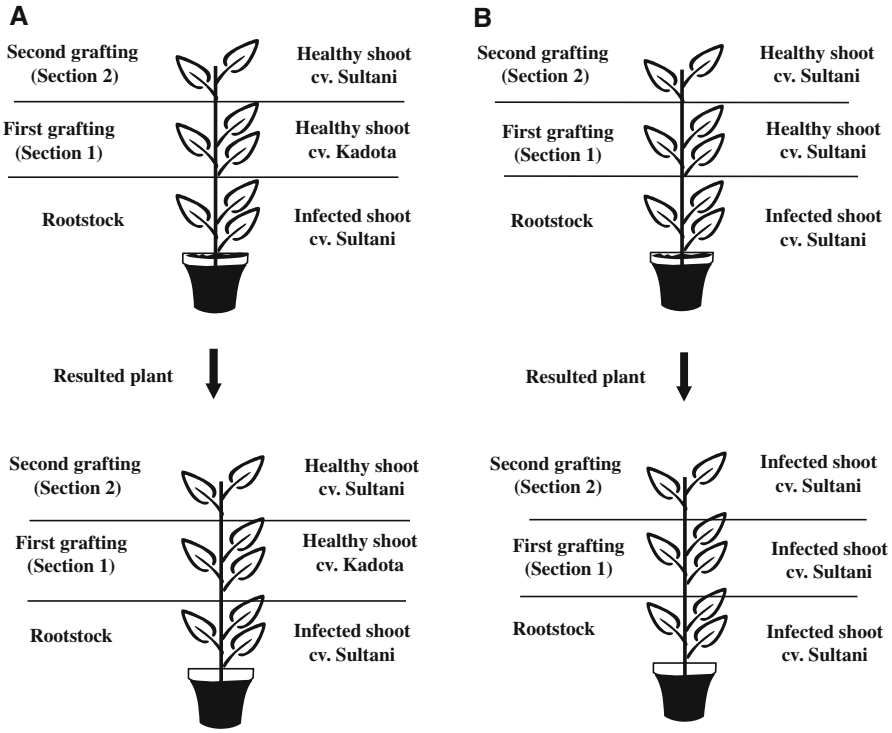

Fig. 2 Diagrammatic figure presenting the double graft experiments. **a** Illustrates the healthy cv. Kadota plant grafted onto infected rootstock cv. Sultani plant [first grafting (section 1)] and healthy cv. Sultani shoot grafted onto healthy cv. Kadota shoot [second grafting (section 2)]. **b** Illustrates the healthy *F. carica* cv. Sultani plant grafted onto infected rootstock *F. carica* cv. Sultani plant [first grafting (section 1)] and the healthy *F. carica* cv. Sultani grafted onto healthy cv. Sultani [second grafting (section 2)]

In the present study, the results (Table 2) of host range indicated that no virus was transmitted mechanically, but was able to systemically infect of *F. carica* cultivars by grafting. The causal agent of fig mosaic disease, which is transmitted by the mite *A. ficus* in the field is uncertain; however, it has common characteristics with high plains virus (Jensen et al. 1996). Its host range appeared to be narrow, mainly restricted to *F. carica* cultivars (Table 2). Virus symptom expression in the field appeared to be systemic and caused malformation of leaves and fruits. Similar mosaic symptoms, malformation and premature fruit dropping were reported in fig plants (Martelli et al. 1993).

Transmission

Data presented in Table 2 indicated that the virus isolate was easily transmissible by grafting to *F. carica* cv. White Aswan and cv. Sultani, but not to *F. carica* cv. Kadota. On the other hand, no virus symptoms were apparently recorded with any mechanical transmission trials. All inoculated hosts remained symptomless even after re-inoculation to new sets of healthy plants.

The data of subsequent grafting of fig cultivars in greenhouse are presented in Table 3. They indicated that no virus inoculation occurred in cv. Kadota plants when grafted onto infected rootstocks of cv. Sultani [Fig. 2a (section 1)], with no symptoms appearing on cv. Sultani [Fig. 2a (section 2)] when grafted onto cv. Kadota [Fig. 2a (section 1)]. On the other hand, the symptoms were developed on cv. Sultani plants [Fig. 2b, (section 1)] when grafted onto infected rootstocks of cv. Sultani. In consequence, the same symptoms were developed on cv. Sultani fig [Fig. 2b (section 2)] after grafted onto cv. Sultani fig. The ELISA applied to plants with or without visual symptoms revealed the presence of virus infection in all cases of cv. Sultani except that grafted on cv. Kadota. These results indicate that the virus particles moved from the infected tissues to healthy ones through grafting. Our results also indicated that the cv. Kadota plants are resistant to viral inoculation and prevent virus transmission (Table 3). Values of ELISA (Table 3) were the same in cv. Kadota plants (section 1) and cv. Sultani plants (section 2) indicative of absence of viral movement and replication in cv. Kadota plant. Application of ELISA to plants that had visual symptoms confirmed the presence of virus infection. Furthermore, plants that were positive by ELISA confirmed for the presence of virus by microscopic investigation, cytopathological studies and RT-PCR analysis employing primers specific to FLMaV-1.

DsRNA analysis and RT-PCR

Nucleic acids suitable for PCR were extracted from virus-infected tissue. Electrophoretic analysis of extracts obtained from the leaf veins of *F. carica* cv. Sultani having symptoms yielded a dsRNA of ca. 19 kbp (Fig. 3). A dsRNA ca. 18 kbp in size was obtained from tissue extracts

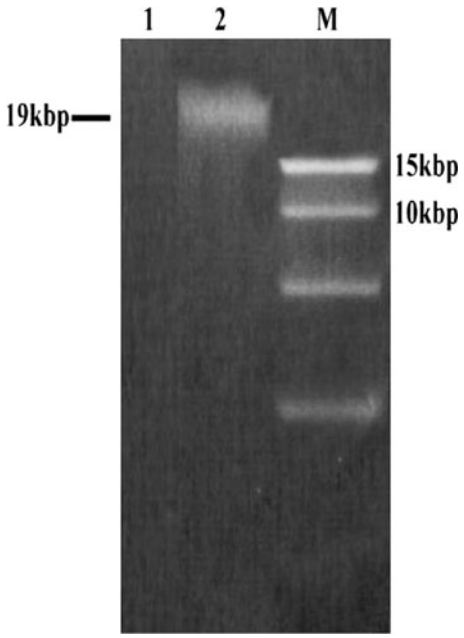

Fig. 3 Agarose gel electrophoresis of dsRNA extracted from symptomatic and symptomless *Ficus carica* cv. Sultani leaves (*Lane 1* and *Lane 2*, respectively, marker *Lane M*). A double-stranded RNA (dsRNA) about 19 kbp only judgment was obtained from the symptomatic fig plant leaves

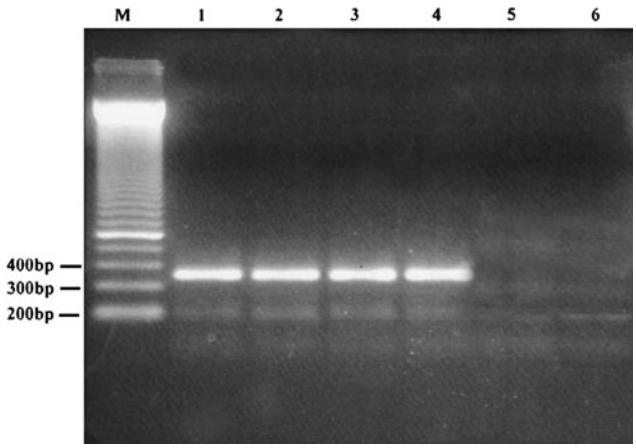

Fig. 4 Agarose gel electrophoresis (1.5%) of reverse-transcriptase polymerase chain reaction (RT-PCR) products amplified from total nucleic acid extracts of leaves of rootstock and grafted plants grown under greenhouse conditions using primers specific for FLMaV-1. The agarose gel lanes represent the following: marker (*Lane M*), infected rootstock cv. Sultani (*Lanes 1* and *2*), cv. Sultani grafted onto infected rootstock (*Lane 3*), cv. Sultani grafted onto infected cv. Sultani (*Lane 4*), healthy cv. Sultani (*Lane 5*) and water control (*Lane 6*). The approximately 350 bp band (*Lanes 1–4*), was indicative of an FLMaV-1-like PCR product

of a fig plant (*F. carica* cv. Sultani) with chlorotic mottling and vein clearing of the leaves (Nahdi et al. 2006). A similar result, a dsRNA ca. 19 kbp in size was reported in a fig tree of Algerian origin (F3) infected by closterovirus

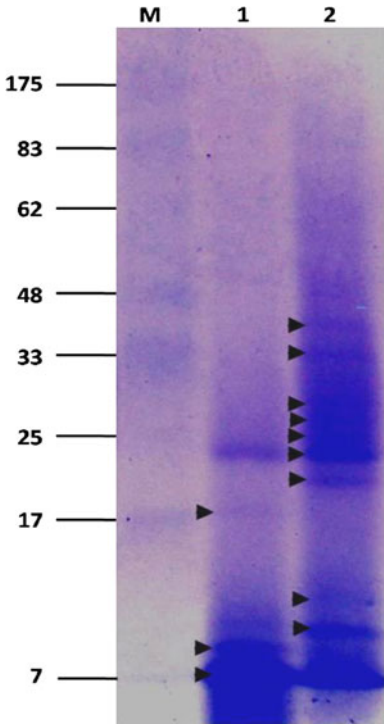

Fig. 5 SDS-PAGE showing changes in protein patterns of fig leaves (*Ficus carica* cv. Sultani) infected with the putative FLMaV-1-like virus identified (*Lane 2*), compared to that of healthy leaves (*Lane 1*). *Lane M* is the protein marker. The supernatant of protein samples containing about 25 µg proteins was loaded onto gel wells. *Arrowheads* are pointing to absent or present of polypeptides due to virus infection

(Elbeaino et al. 2007). Using FLMaV-1-specific primers (Elbeaino et al. 2006) that amplify phosphate motifs 1 and 2 of the heat shock-protein 70 homologue (Hsp70h) gene of the family *Closteroviridae*, amplicons of the expected size of 350 bp were obtained from samples infected with the identified virus (Fig. 4). All symptomatic samples of rootstock and grafted fig plants of cv. Sultani had the same patterns (Fig. 4). Previously published data indicated a number of taxonomically different viruses found in *F. carica* trees with symptoms in the family *Closteroviridae* (Elbeaino et al. 2006, 2007).

Protein electrophoretic patterns

The electrophoretic pattern of leaf proteins from *F. carica* cv. Sultani plants infected with the virus showed many changes and modifications in the protein bands (Fig. 5). Viral infections resulted in appearance of new polypeptides of about 13, 19, 21, 25, 27, 29, 31 and 41 kDa, while polypeptides of about 9 and 17 kDa have disappeared. Some bands of newly synthesized polypeptides resulted from viral infection showed a low density. Accumulation and induction of pathogenesis-related proteins (PRs) were

Table 4 Levels of photosynthetic pigments (mg g^{-1} FW) in healthy and virus-infected leaves of *Ficus carica* cv. Sultani

	Chl *a* $M \pm$ SD	Chl *b* $M \pm$ SD	*Carotenoids* $M \pm$ SD	*Chl a/b* ratio	Total	%
Health leaves	1.26 ± 0.15	0.87 ± 0.07	0.29 ± 0.04	1.45	2.42	100.00
Infected leaves	0.85 ± 0.07	0.51 ± 0.06	0.26 ± 0.03	1.66	1.62	66.94

The values are means (*M*) of nine replicates ± standard deviation (SD)

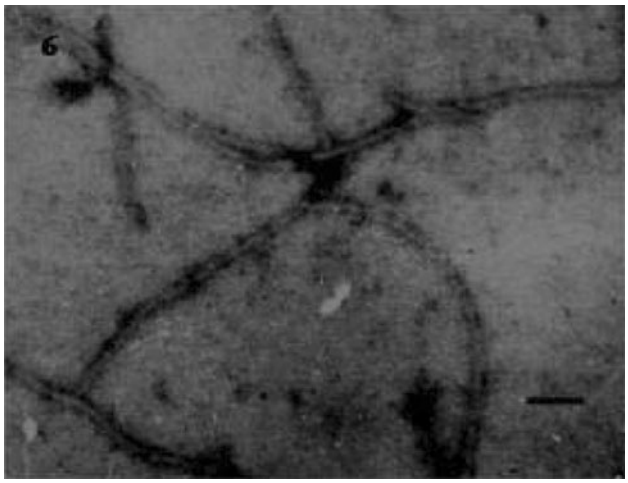

Fig. 6 Negative stained preparation of the sap of infected *F. carica* cv. Sultani leaves showing broken filamentous particles. *Bar* 60 nm

reported in other works (Radwan et al. 2007; Elvira et al. 2008; Guevara-Morato et al. 2010). Plants responded to pathogen attack by formation of new families of proteins called PRs. Although some of them are implicated in plant defence, they have not been identified because of their antimicrobial activity, but only because of their accumulation in infected plants (van Loon 1985; van Loon 1997). In the present study, the formation of new polypeptides is probably an indicator of plant resistance towards the virus infection and reflects the physiological status of the plant. Further studies will be needed to study proteins and enzymes involved in resistance and susceptible fig plant defences against virus infection.

Photosynthetic pigments

Viral infection decreased the photosynthetic pigment contents of *F. carica* leaves (Table 4). Contents of chl *a*, chl *b* and carotenoids of *F. carica* cv. Sultani leaves decreased by 32.54, 41.79, and 10.34%, respectively, in response to viral infection. These data indicate that chl *b* affected virus infection to a greater extent than chl *a* and carotenoids. The most commonly observed symptoms characteristic to specific host–virus interactions, were often accompanied by a decrease in chl contents, photosynthetic rate, delayed chlorophyll biosynthesis and inhibition of the electron transport on the donor side of PSII (Almási et al. 2000; Arias et al. 2003; Synková et al. 2006; Radwan et al. 2007).

Electron microscopy and cell ultrastructure

Filamentous particles ~1.8 µm long and ~21 nm in diameter were seen in purified leaf veins from symptomatic sources of *F. carica* cv. Sultani (Fig. 6). However, no filamentous virus particles or membrane-bound bodies typically associated with fig mosaic were detected in mesophyll cells. Filamentous closterovirus-like particles up to 2,100 nm in length and with distinct cross banding were observed in fig leaf dips (Elbeaino et al. 2007). On the other hand, Dolja (2003) reported that the virions of *Beet yellow virus* (genus Closterovirus) are flexuous filaments of ~1,300 nm in length and ~12 nm in diameter and made up of a ~15.5 kb RNA and five proteins.

In healthy plants of *F. carica* cv. Sultani (Fig. 7a), the chloroplasts were characterized by an accumulation of starch granules, well-displayed grana thylakoid and condensed stroma matrix. In response to viral infection, starch granules within chloroplasts were partially or totally disappeared depending on the severe damage (Fig. 7b–d). Virus inclusions bodies were not visible in the cytoplasm and any other cell organelles of mesophyll cells. The chloroplast envelope partially or totally disappeared and the internal network of grana and stroma thylakoids were almost degenerated. Some remaining grana thylakoids were dispersed in the cytoplasm (Fig. 7b, c). With severe virus infection, the grana and stroma thylakoids turned to spherical body's like-chromplasts (Fig. 7d). Deterioration of chloroplast ultrastructure and pigment composition can be attributed to the damage caused mostly to PSII due to viral infection (Nanda and Biswal 2008; Díaz-Vivancos et al. 2008). In addition to chloroplast deformation, the nuclear membrane appeared to be affected in virus-infected leaves (Fig. 7d).

Catalase and peroxidase activity

Catalase activity was declined by 36%, while peroxidase activity increased by 106% in the infected leaves compared with those of healthy ones (Table 5). Production of ROS is one of the responses of plant tissues to the attack of

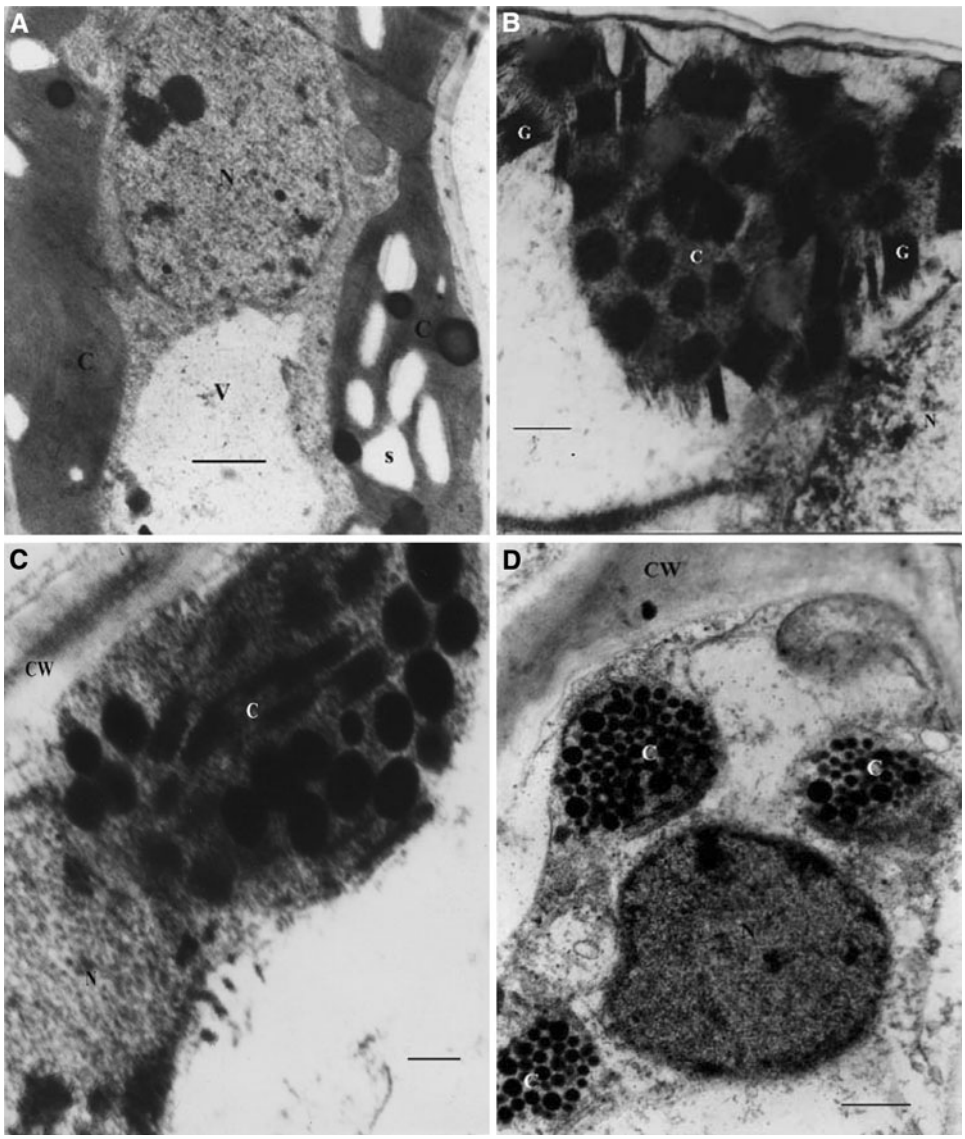

Fig. 7 Electron micrographs of portions of mesophyll cell ultrastructure of healthy *Ficus carica* cv. Sultani (**a**) and virus infected leaves (**b–d**). In healthy leaves, the micrograph shows chloroplasts (*C*), nucleus (*N*) having a normal organization. Many starch grains (*s*) are showing within chloroplasts. Ultrastructural disorganization of cell organelles in virus-infected leaves is clearly visible: the grana thylakoids of chloroplasts are degenerated and have turned to spherical bodies (**d**). The envelope and the internal network of thylakoid membranes of chloroplasts are almost degenerated. Some grana of chloroplasts are scattered in the cytoplasm. The nuclear envelope is also deformed (**b–d**). *Scale bars* 1,000, 500, 500, and 800 nm, respectively

Table 5 Levels of catalase and peroxidase activities in healthy and virus-infected leaves of *Ficus carica* cv. Sultani

	Catalase activity (μM H_2O_2 min^{-1} g FW)		Peroxidase activity (μM Guaiacol min^{-1} g FW)	
	Mean ± SD	%	Mean ± SD	%
Healthy leaves	55.33 ± 8.32	100	96.67 ± 10.41	100
Infected leaves	35.33 ± 4.17	64	200.17 ± 21.79	206

The values are means (*M*) of nine replicates ± standard deviation (SD)

Table 6 Levels of MDA and total phenolics in healthy and virus-infected leaves of *Ficus carica* cv. Sultani

	MDA (μM g^{-1}FW)		Total phenolics (μM Gallic acid g^{-1}DW)	
	Mean ± SD	%	Mean ± SD	%
Healthy leaves	43.66 ± 2.08	100	32 ± 5.00	100
Infected leaves	50.66 ± 3.05	115	41 ± 5.05	129

The values are means (*M*) of nine replicates ± standard deviation (SD)

pathogens and elicitors (Wojtaszek 1997; Otulak and Garbaczewska 2010; Radwan et al. 2010). Declined CAT and enhanced POX activities are shown to be a response of plants towards pathogen stress situations (Chen et al.1993; Clarke et al. 2002). POX is considered to be one of the antioxidant enzymes that are involved in the plant defence response to pathogen attack; it is often the first enzyme to show changes in its activity under stress (Milavec et al. 2001). In our previous work (Radwan et al. 2006), we found increase in POX and accumulation of ROS in *C. pepo* due to ZYMV infection. ROS accumulation causes oxidative damage through actions such as lipid peroxidation and membrane destruction. ROS is proposed to be responsible for chlorophyll degradation and increase of POX levels during senescence (Kuroda et al. 1990; Riedle-Bauer 2000).

Phenolics and lipid peroxidation

In response to virus infection, an elevated level of phenolics was detected in infected fig leaves (Table 6). This increase reaches to 29% as compared to that of healthy leaves. Increasing phenolic compounds in response to biotic stress might act as free radical scavengers and protect cells from their oxidative toxicity (Yalpani et al. 1993). Membrane lipid peroxidation in the leaves was assessed by determining the accumulation of thiobarbituric acid reactants (TBARS). In response to virus infection, an elevated level of lipid peroxidation was observed in infected leaves. This increase is ca. 15% as compared to that of healthy leaves (Table 6). Several stresses have been described as inducers of ROS in plants, which attack the polyunsaturated fatty acid components of membrane lipids resulting in lipid peroxidation. This process promotes the disruption of physical and functional properties of membranes (Chaoui et al. 1997; Li and Burritt 2003; Radwan et al. 2006).

In conclusion, results of the present study allow us to draw the following points. The identified Egyptian FLMaV-1-like virus caused leaf mosaic and chlorotic symptoms and probably belongs to genus *Closterovirus*. This is supported by the analysis of viral genomic RNA. A dsRNA, about 19 kbp was obtained and a cDNA fragment (350 bp) was amplified by RT-PCR from the tissue extract of fig symptomatic plants. Newly synthesized polypeptides appeared, while others disappeared in virus-infected leaves reflecting the formation of pathogenesis related proteins. Ultrastructure and physiological analyses indicated that chloroplasts and their components were the main sites of virus action. Also, viral infection altered other aspects of the fig plant physiology, including the up-regulation of enzymes involved in antioxidant metabolism, accumulation of MDA and phenolics.

References

Almási A, Apatini D, Bóka K, Böddi B, Gáborjányi R (2000) BSMV infection inhibits chlorophyll biosynthesis in barley plants. Physiol Mol Plant Pathol 56:227–233

Appiano A, Conti M, Zini N (1995) Cytopathological study of the double-membrane bodies occurring in fig plants affected by fig mosaic disease. Acta Hortic 386:585–592

Arias MC, Lenardon S, Taleisnik E (2003) Carbon metabolism alterations in sunflower plants infected with the *Sunflower chlorotic mottle virus*. J Phytopathol 151:267–273

Bolwell GP, Bindschedler LV, Blee KA, Butt VS, Davies DR, Gardner SL, Gerrish C, Minibayeva F (2002) The apoplastic oxidative burst in response to biotic stress in plants: a three-component system. J Exp Bot 53:1367–1376

Buchanan-Wollaston V (1997) The molecular biology of leaf senescence. J Exp Bot 48:181–191

Cai YZ, Luo Q, Sun M, Corke H (2004) Antioxidant activity and phenolic compounds of 112 traditional Chinese medicinal plants associated with anticancer. Life Sci 74:2157–2184

Candela ME, Munoz R, Alcázar MD, Espín A (1994) Isoperoxidase involvement in the resistance of *Capsicum annuum* to infection by cucumber mosaic virus. J Plant Physiol 143:213–217

Chandlee JM, Scandalios JG (1984) Analysis of variants affecting the catalase development program in maize scutellum. Theor Appl Genet 69:71–77

Chaoui A, Mazhoudi S, Ghorbal MH, El Ferjani E (1997) Cadmium and zinc induction of lipid peroxidation and effects on antioxidant enzyme activities in bean (*Phaseolus vulgaris* L.). Plant Sci 127:139–147

Chen ZX, Silva H, Klessig DF (1993) Active oxygen species in the induction of plant systematic acquired-resistance by salicylic acid. Science 262:1883–1886

Clark MF, Adams AN (1977) Characteristics of the microplate method of enzyme-linked immunosorbent assay for the detection of plant viruses. J Gen Virol 34:475–483

Clarke SF, Guy PL, Burritt DJ, Jameson PE (2002) Changes in the activities of antioxidant enzymes in response to virus infection and hormone treatment. Physiol Plant 114:157–164

Costa RM, Magalhães AS, Pereira JA, Andrade PB, Valentão P, Carvalho M, Silva BM (2009) Evaluation of free radical-scavenging and antihemolytic activities of quince (*Cydonia oblonga*) leaf: a comparative study with green tea (*Cammelia sinensis*). Food Chem Toxicol 47:860–865

Dai GH, Andary C, Cosson-Mondolot L, Boubals D (1994) Polyphenols and resistance of grapevines to downy mildew. Acta Hortic 381:763–766

Díaz-Vivancos P, Clemente-Moreno JM, Rubio M, Olmos E, García JA, Martínez-Gómez P, Hernández JA (2008) Alteration in the chloroplastic metabolism leads to ROS accumulation in pea plants in response to plum pox virus. J Exp Bot 59:2147–2160

Dolja VV (2003) *Beet yellows virus*: the importance of being different. Mol Plant Pathol 4:91–98

Elbeaino T, Digiaro M, De Stradis A, Martelli GP (2006) Partial characterisation of a closterovirus associated with a chlorotic mottling of fig. J Plant Pathol 88:187–192

Elbeaino T, Digiaro M, De Stradis A, Martelli GP (2007) Identification of a second member of the family *Closteroviridae* in mosaic-diseased figs. J Plant Pathol 89:119–124

Elbeaino T, Digiaro M, Alabdullah A, De Stradis A, Minafra A, Mielke N, Castellano MA, Martelli GP (2009a) A multipartite single-stranded negative-sense RNA virus is the putative agent of fig mosaic disease. J Gen Virol 90:1281–1288

Elbeaino T, Digiaro M, Martelli GP (2009b) Complete nucleotide sequence of four RNA segments of fig mosaic virus. Arch Virol 154:1719–1727

Elvira MI, Galdeano MM, Gilardi P, García-Luque I, Serra MT (2008) Proteomic analysis of pathogenesis-related proteins (PRs) induced by compatible and incompatible interactions of pepper mild mottle virus (PMMoV) in *Capsicum chinense* L3 plants. J Exp Bot 59:1253–1265

Falk BW, Tsai JH (1984) Identification of single and double stranded RNAs associated with maize stripe virus. Phytopathol 64:909–915

FAO (2006) FAOSTAT agricultural data. http://faostat.fao.org/site/408/default.aspx. Accessed Aug 2006

Guevara-Morato MA, de Lacoba MG, García-Luque I, Serra MT (2010) Characterization of a pathogenesis-related protein 4 (PR-4) induced in *Capsicum chinense* L3 plants with dual RNase and DNase activities. J Exp Bot 61:3259–3271

Harper K, Kreamer R (1995) Hybridization detection of insect-transmitted plant viruses with digoxigenin-labeled probes. Plant Dis 78:563–567

Hernández JA, Almansa MS (2002) Short-term effects of salt stress on antioxidant systems and leaf water relations of pea leaves. Physiol Plant 115:251–257

Hernández JA, Rubio M, Olmos E, Ros-Barcelo A, Martinez-Gomez P (2004) Oxidative stress induced by long-term plum pox virus infection in peach (*Prunus persica*). Physiol Plant 122:486–495

Jensen SG, Lane LC, Seifers DL (1996) A new disease of maize and wheat in the high plains. Plant Dis 80:1387–1390

Karasev AV (2000) Genetic diversity and evolution of closteroviruses. Annl Rev Phytopathol 38:293–324

Kofalvi SA, Nassuth A (1995) Influence of wheat streak mosaic virus infection on phenylpropanoid metabolism and the accumulation of phenolics and lignin in wheat. Physiol Mol Plant Pathol 47:365–377

Kuroda M, Ozawa T, Imagava H (1990) Changes in chloroplast peroxidase activities in relation to chlorophyll loss in barley leaf segments. Physiol Plant 80:555–560

Laemmli UK (1970) Cleavage of structural proteins during the assembly of the head of bacteriophage T4. Nature 227:680–685

Léon J, Lawton MA, Raskin I (1995) Hydrogen peroxide stimulates salicylic acid biosynthesis in tobacco. Plant Physiol 108:1673–1678

Li Z, Burritt DJ (2003) The influence of *Cocksfoot mottle* virus on antioxidant metabolism in the leaves of *Dactylis glomerata* L. Physiol Mol Plant Pathol 62:285–295

Lichtenthaler HK (1987) Chlorophylls and carotenoids–pigments of photosynthetic biomembranes. In: Colowick SP, Kaplan NO (eds) Methods in enzymology, vol 148. Academic Press, San Diego, pp 350–382

Lin CC, Kao CH (2000) Effect of NaCl stress on H_2O_2 metabolism in rice leaves. Plant Growth Regul 30:151–155

Mars M (2003) Fig (*Ficus carica* L.) genetic resources and breeding. Acta Hortic 605:19–27

Martelli GP, Castellano MA, Lafortezza R (1993) An ultrastructural study of fig mosaic. Phytopathol Mediterr 32:33–43

Milavec M, Ravnikar M, Kovač M (2001) Peroxidases and photosynthetic pigments in susceptible potato infected with potato virus Y^{NTN}. Plant Physiol Biochem 39:891–898

Nahdi S, Elbeaino T, Digiaro M, Martelli GP (2006) First record of fig leaf mottle-associated virus 1 in Tunisia. J Plant Pathol 88:S70

Nanda RM, Biswal B (2008) Biotic stress induced demolition of thylakoid structure and loss in photoelectron transport of chloroplasts in papaya leaves. Plant Physiol Biochem 46:461–468

Oliveira AP, Valenão P, Pereira JA, Silva BM, Tavares F, Andrade PB (2009) *Ficus carica* L.: Metabolic and biological screening. Food Chem Toxicol 47:2841–2846

Otulak K, Garbaczewska G (2010) Localisation of hydrogen peroxide accumulation during *Solanum tuberosum* cv. Rywal hypersensitive response to Potato virus Y. Micron 41:327–335

Polle A, Otter T, Seifert F (1994) Apoplastic peroxidases and lignifications in needles of Norway Spruce *Picea abies* L. Plant Physiol 106:53–60

Radwan DEM, Fayez KA, Mahmoud SY, Hamad A, Lu G (2006) Salicylic acid alleviates growth inhibition and oxidative stress caused by zucchini yellow mosaic virus infection in *Cucurbita pepo* leaves. Physiol Mol Plant Pathol 69:172–181

Radwan DEM, Fayez KA, Mahmoud SY, Hamad A, Lu G (2007) Physiological and metabolic changes of *Cucurbita pepo* leaves in response to zucchini yellow mosaic virus (ZYMV) infection and salicylic acid treatments. Plant Physiol Biochem 45:480–489

Radwan DEM, Fayez KA, Mahmoud SY, Hamad A, Lu G (2010) Modifications of antioxidant activity and protein composition of bean leaf due to Bean yellow mosaic virus infection and salicylic acid treatments. Acta Physiol plant 32:891–904

Rahoutei J, Garcia-Luque I, Baron M (2000) Inhibition of photosynthesis by viral infection: effect on PSII structure and function. Physiol Plant 110:286–292

Reinero A, Beachy RN (1989) Reduced photosystem II activity and accumulation of viral coat protein in chloroplasts of leaves infected with tobacco mosaic virus. Plant Physiol 89:11–16

Riedle-Bauer M (2000) Role of reactive oxygen species and antioxidant enzymes in systemic virus infections of plants. J Phytopathol 148:297–302

Saldarelli P, Minafra A, Martelli GP, Walter B (1994) Detection of grapevine leafroll associated closterovirus III by molecular hybridization. Plant Pathol 43:91–96

Serrano L, Ramon J, Segarra J, Medina V, Achón MA, López M, Juárez M (2004) New approach in the identification of the causal agent of fig mosaic disease. Acta Hortic 657:559–566

Spurr AR (1969) A low viscosity epoxy resin embedding medium for electron microscopy. J Ultra Res 26:31–43

Stover Ed, Aradhya M, Ferguson L, Crisosto CH (2007) The fig: overview of an ancient fruit. Hortic Sci 42:1083–1087

Synková H, Semorádová Š, Schnablová R, Müller K, Pospíšilová J, Ryšlavá H, Malbeck J, Čeřovská N (2006) Effects of biotic stress caused by Potato virus Y on photosynthesis in *ipt* transgenic and control *Nicotiana tabacum* L. Plant Sci 171:607–616

Técsi L, Smith AM, Maule AJ, Richard C (1996) A spatial analysis of physiological changes associated with infection of cotyledons of marrow plants with cucumber mosaic virus. Plant Physiol 111:975–985

Tzanetakis IE, Martin RR (2007) Strawberry chlorotic fleck: identification and characterization of a novel *Closterovirus* associated with the disease. Virus Res 124:88–94

van Loon LC (1985) Pathogenesis-related proteins. Plant Mol Biol 4:111–116

van Loon LC (1997) Induced resistance in plants and the role of pathogenesis-related proteins. Eur J Plant Pathol 103:753–765

Veberic R, Colaric M, Stampar F (2008) Phenolic acids and flavonoids of fig fruit (*Ficus carica* L.) in the northern Mediterranean region. Food Chem 106:153–157

Walia JJ, Salem NM, Falk BW (2009) Partial sequence and survey analysis identify a multipartite, negative-sense RNA virus associated with fig mosaic. Plant Dis 93:4–10

Wojtaszek P (1997) Oxidative burst: an early plant response to pathogen infection. Biochem J 322:681–692

Yalpani N, León J, Lawton MA, Raskin I (1993) Pathway of salicylic acid biosynthesis in healthy and virus-inoculated tobacco. Plant Physiol 103:315–321